Developmental and Comparative Immunology 104 (2020) 103563

Contents lists available at ScienceDirect

Developmental and Comparative Immunology

journal homepage: www.elsevier.com/locate/devcompimm

# A membrane-bound dopamine β-hydroxylase highly expressed in granulocyte of Pacific oyster *Crassostrea gigas*

Meijia Li[a,c], Miren Dong[c], Weilin Wang[b,c], Huan Li[c], Zhaoqun Liu[c], Lingling Wang[b,c,d,e], Kejian Wang[a], Linsheng Song[b,c,d,*]

[a] State Key Laboratory of Marine Environmental Science, College of Ocean & Earth Science, Xiamen University, Xiamen, 361102, China
[b] Functional Laboratory of Marine Fisheries Science and Food Production Process, Qingdao National Laboratory for Marine Science and Technology, Qingdao, 266071, China
[c] Liaoning Key Laboratory of Marine Animal Immunology & Disease Control, Dalian Ocean University, Dalian, 116023, China
[d] Liaoning Key Laboratory of Marine Animal Immunology, Dalian Ocean University, Dalian, 116023, China
[e] Dalian Key Laboratory of Prevention and Control of Aquatic Animal Diseases, Dalian Ocean University, Dalian, 116023, China

ARTICLE INFO

*Keywords:*
*Crassostrea gigas*
Dopamine β-hydroxylase
Granulocytes
Immune regulation

ABSTRACT

Dopamine β-hydroxylase (DBH) is one of key rate-limiting enzymes converting dopamine to norepinephrine. It locates not only in catecholaminergic neuron system, but also in immunocytes and plays roles in the immune response of vertebrates. However, the knowledge about the function of DBH in immune system is still very limited in invertebrates. In the present study, the DBH gene family with seven members was screened from *Crassostrea gigas* genome, and their mRNA expressions in various tissues were recorded. Among them, one DBH (designated *Cg*DBH-1) with high expression level in oyster hemocytes was further characterized. The deduced amino acid sequence of *Cg*DBH-1 was predicted to contain a transmembrane domain and shared 30.1% and 30.9% similarity with that in *Mus musculus* and *Homo sapiens*, respectively. *Cg*DBH-1 was closely clustered with DBH from *Aplysia californica* in the phylogenetic tree. The recombinant protein of *Cg*DBH-1 (r*Cg*DBH-1) exhibited significant enzymatic activity ($0.54 \pm 0.019$ pmol $L^{-1}$ $min^{-1}$) to synthesize norepinephrine. Importantly, the mRNA transcript of *Cg*DBH-1 was highly expressed in oyster hemocytes, and the highest expression level was observed in granulocytes among the three types of hemocytes, which was 8.18-fold ($p < 0.01$) of that in agranulocytes. Moreover, the expression of *Cg*DBH-1 in hemocytes was significantly increased at the late stage of immune response. The *Cg*DBH-1 protein was mainly co-localized with the granules and endoplasmic reticulum (ER) of granulocytes. These results collectively suggested that *Cg*DBH-1, as a novel molluscan norepinephrine synthesizing enzyme highly expressed in granulocytes, involved in the late-stage immune response of oysters, which provided vital insight to understand the crosstalk between neuroendocrine and immune systems in invertebrates.

## 1. Introduction

The bi-directional communication of the neuroendocrine and immune systems (NEI systems) plays a vital role in maintaining allostasis of organisms (Reardon et al., 2018; Verburg-van Kemenade et al., 2017). Traditionally, hormones or neurotransmitters could be synthesized and released from neuroendocrine system of organisms, and modulate immune activities through their specific receptors expressed in immunocytes. Immune system could produce kinds of cytokines to regulate the activities of nervous system as well (Liu et al., 2018a; Malagoli and Ottaviani, 2017; Raison et al., 2006). Recently, an increasing number of studies have reported that except this kind of classical interactions, novel regulation model also exists in specific immunocytes of vertebrates, in which hormones or neurotransmitters could be released directly from immunocytes and function on themselves in an autocrine or paracrine pattern (Fujii et al., 2017). It has been realized that the immunocytes-derived neurotransmitters play important roles in health and disease of human (Reardon et al., 2018). However, little is known about hormones or neurotransmitters synthesized in invertebrate immunocytes and their physical functions.

Among the neuroendocrine-immune regulatory network, catecholamines (CAs), including dopamine (DA), norepinephrine (NE) and epinephrine (E), were regarded as one kind of the most important neurotransmitters in Chordata (Sabban and Kvetňanský, 2001). These

* Corresponding author. Dalian Ocean University, Dalian, 116023, China.
*E-mail address:* lshsong@dlou.edu.cn (L. Song).

https://doi.org/10.1016/j.dci.2019.103563
Received 23 September 2019; Received in revised form 26 November 2019; Accepted 27 November 2019
Available online 28 November 2019
0145-305X/ 

neurotransmitters are related with each other in biosynthetic processes. Dopamine β-hydroxylase (DBH), as a key rate-limiting enzyme in the CAs biosynthetic pathway, can convert the DA to NE in the presence of molecular oxygen and ascorbic acid (Kvetňanský et al., 2009). The classical structure of DBH includes N-terminal signal peptide, a DOMON domain and two catalytic $Cu_H$ and $Cu_M$ domains (Vendelboe et al., 2016). DBH could control the concentrations of DA and NE and regulate their balance in nervous system, by which it involves in various physiological or neurological diseases, such as Alzheimer's disease, Parkinson's disease and Schizophrenia (Tang et al., 2018; Trillo et al., 2013). DBH also plays important modulatory roles in immune defense reactions. For example, the mice of DBH knocked-out were more susceptible to infection and suffered an impaired T cell function and Th1 T cell-dependent-IgG2a antibody production (Alaniz et al., 1999). Besides, DBH has been discovered to function in immune cells of specific types. For example, DBH in phagocytes of mice could be significantly induced by lipopolysaccharide (LPS) stimulation, and promote the *de novo* production of NE which could further participate in inflammatory regulation in an autocrine/paracrine manner but independent of sympathetic nerve modulations (Flierl et al., 2007).

So far, some DBHs have been identified in invertebrates, such as in *Ciona savignyi* (Kimura et al., 2003), *Trichoplax* (Srivastava et al., 2008) and *Aiptasia pallida* (Westfall et al., 2000), and their immunomodulation functions were also explored. In scallop *Chlamys farreri*, the mRNA expression of DBH in hemocytes could be significantly induced after LPS stimulation (Zhou et al., 2011). In *Litopenaeus vannamei*, the DBH-depleted organisms exhibited immunosuppression and decreased survival ratio to *Vibrio alginolyticus* infection (Cheng et al., 2017). In oyster *Crassostrea gigas*, the enzyme activity of DBH could be detected in cell lysates of hemocytes, and the hemocytes-derived NE could execute a negative regulation on hemocyte phagocytosis and synthesis of immune effectors (Liu et al., 2018b). However, no given DBH executing these functions is demonstrate in oyster until now. In oyster *C. gigas*, three types of hemocytes have been identified and the granulocytes were demonstrated to be the main immunocompetent hemocytes (Wang et al., 2017). Whether the NE synthesized and functioned in hemocytes of specific types is yet obscure.

The Pacific oyster *C. gigas* is one of most important marine mollusks and contributes greatly to the aquaculture industry worldwide (Zhang et al., 2016). As filter feeders, oysters are exposed to high microbial pathogen loads and experience the ever-changing environment (Evans et al., 2017). Understanding the intrinsic immune modulatory manner of oysters is quite important for providing efficient strategies to prevent disastrous disease. Though plenty of progresses about immune defense mechanisms of marine invertebrates have been achieved in the past two decades (Lacoste et al., 2001), the neuroendocrine regulation on immune response is still waiting to be uncovered. In the present study, the dopamine β-hydroxylase family (designated as *Cg*DBH) was screened from *C. gigas* genome with the purposes to (1) analyze the memberships of DBH family and their expression patterns, (2) identify the DBH (*Cg*DBH-1) functioning in hemocytes and its expression patterns in different tissues and hemocyte sub-types, (3) explore the molecular features and enzyme activity of *Cg*DBH-1, and (4) investigate the possible regulation role of *Cg*DBH-1 in the immune response of oysters.

## 2. Materials and methods

### 2.1. Animals

Pacific oysters (*C. gigas*, about two years old) were collected from a local farm in Dalian, Liaoning province, China, and acclimatized in tanks with filtered and aerated seawater (about 15–20 °C) for at least one week before processing.

### 2.2. LPS stimulation and tissues collection

One hundred and sixty oysters were randomly selected and sawed in the closed side of the oyster shell adjacent to the adductor muscle. After acclimating for another one week, those oysters were randomly divided into two groups (80 individuals in each group) and received an injection of 100 μL phosphate buffer saline (PBS) (0.27 g $L^{-1}$ $KH_2PO_4$, 3.58 g $L^{-1}$ $Na_2HPO_4{\cdot}12H_2O$, 8.00 g $L^{-1}$ NaCl and 0.20 g $L^{-1}$ KCl, pH 7.4) or LPS (0.5 g $L^{-1}$ in PBS, Sigma), respectively. After injection, those oysters were returned to filtered seawater immediately, and then nine individuals were randomly sampled in each treatment group at 0, 3, 6, 12, 24, 48, 72 and 96 h post injection.

Nine oysters were equally divided into three parallels with three individuals in each parallel, and the hemolymphs were individually collected and pooled together in each parallel. Then the hemolymphs were centrifuged at 800 *g*, 4 °C for 10 min to harvest hemocytes. Those enriched hemocytes were dissolved in Trizol reagent, frozen with liquid nitrogen immediately and stored at −80 °C for the following RNA isolation. Besides, tissues including adductor muscle, labial palp, gills, gonad, hemocytes, mantle, visceral ganglia and hepatopancreas, were collected from nine untreated oysters, and male and female individuals were not distinguished as comparable expression levels of *Cg*DBH-1 were indicated according to oyster genome data (Zhang et al., 2012). These samples were also kept in Trizol reagent at −80 °C for the subsequent RNA isolation.

### 2.3. Density gradient centrifugation for sub-types separation of hemocytes

In order to separate the three sub-types of oyster hemocytes, the density gradient centrifugation assay was carried out according to the previous description (Wang et al., 2017). Briefly, the commercial Percoll solution (Sigma) was adjusted to 1000 mOsm by adding 10 × saline (202 g $L^{-1}$ NaCl, 5 g $L^{-1}$ KCl, 6 g $L^{-1}$ $CaCl_2$, 1 g $L^{-1}$ $MgSO_4$ and 39 g $L^{-1}$ $MgCl_2$) at the ratio of 9:1 (v/v), which was regarded as 100% Percoll gradient. Subsequently, 55% and 30% (v/v) Percoll gradients were prepared with 100% Percoll and 1 × saline (20.2 g $L^{-1}$ NaCl, 0.5 g $L^{-1}$ KCl, 0.6 g $L^{-1}$ $CaCl_2$, 1.0 g $L^{-1}$ $MgSO_4$ and 3.9 g $L^{-1}$ $MgCl_2$). The hemocytes from untreated oysters suspended in modified Alsever's solution (MAS, 20.8 g $L^{-1}$ glucose, 8.0 g $L^{-1}$ sodium citrate, 3.36 g $L^{-1}$ EDTA and 22.5 g $L^{-1}$sodium chloride, pH 7.5) (about $10^7$ cells $mL^{-1}$) were layered onto the top of a Percoll gradient. After centrifugation at 600 *g*, 4 °C for 15 min, the hemocytes were presented at the bottom, the interface and the upper layer of the 55%/30% gradient, respectively, and those hemocytes in different sub-populations were separately collected and washed with modified L15 medium (L15 medium supplemented with 10 × saline at the ratio of 9:1 (v/v)). After that, the collected hemocytes in each layer were layered onto the top of fresh Percoll gradients for the second separation as former description. Then the hemocytes in the bottom, interface and upper layer of Percoll gradient were collected as granulocytes, semi-granulocytes and agranulocytes, respectively, which were immediately frozen in liquid nitrogen with Trizol regent for following RNA isolation.

### 2.4. RNA extraction and cDNA synthesis

Total RNA in collected samples was extracted using Trizol (Invitrogen) according to the manufacturer's protocol. Briefly, oyster tissues (50–100 mg) were homogenized in Trizol reagent, and then chloroform was added into the tissue homogenate to separate total RNA. After being precipitated from aqueous phase using isopropanol, the total RNA was cleaned by 75% ethanol. Finally, the total RNA was resuspended by RNase-free water and prepared for cDNA synthesis. The cDNA synthesis was performed by one-step gDNA removal and cDNA synthesis supermix kit (Transgen) in accordance with the manufacturer's instruction. After reverse transcription, the cDNA mix was stored at −80 °C for gene clone and quantitative real-time PCR.

**Table 1**
Information of DBH genes screened from oyster *C. gigas* genome.

| NO. | Gene ID | Amino acids | Structure domains of protein |
|---|---|---|---|
| ***Cg*DBH-1** | CGI_10026674 | 568 | Signal peptide + $Cu_H$ + $Cu_M$ + transmembrane |
| ***Cg*DBH-2** | CGI_10001849 | 495 | $Cu_H$ + $Cu_M$ |
| ***Cg*DBH-3** | CGI_10002524 | 522 | $Cu_H$ + $Cu_M$ |
| ***Cg*DBH-4** | CGI_10027734 | 558 | DOMON + $Cu_H$ + $Cu_M$ |
| ***Cg*DBH-5** | CGI_10020572 | 725 | Signal peptide + DOMON + $Cu_H$ + $Cu_M$ + DOMON |
| ***Cg*DBH-6** | CGI_10024061 | 613 | Signal peptide + DOMON + $Cu_H$ + $Cu_M$ |
| ***Cg*DBH-7** | CGI_10013490 | 850 | DOMON + $Cu_H$ + $Cu_M$ + DOMON |

### 2.5. Genomic screening of DBH gene family, gene clone and sequence analysis

The DBH genes were searched from annotated oyster genome (Zhang et al., 2012), and all the genes annotated as dopamine β-hydroxylase were selected as members of DBH family. The amino acid sequences of these genes were retrieved from OysterBase (http://www.oysterdb.com), and further analyzed for their domain structures by the simple modular architecture research tool (SMART) version 8.0 (http://smart.embl-heidelberg.de/). Their expression data (RPKM value, Reads Per Kilobase per Million mapped reads) were also retrieved from supplementary information of oyster genome to analyze their expression patterns in different adult tissues.

The nucleotide sequence of a *Cg*DBH-1 gene (CGI_10026674) was retrieved from OysterBase and a pair of specific primers P2 and P3 (Table 2) was designed to clone the coding sequence of *Cg*DBH-1. The PCR product was gel-purified and cloned into the pMD19-T simple vector (Takara), and then three positive clones were selected and sequenced with primers P4 and P5 (Table 2). The nucleotide sequence was deduced as amino acid sequence by Primer Premier 5, and the amino acid sequence was analyzed with the Expert Protein Analysis System (http://www.expasy.org) and the protein domain was predicted with SMART version 8.0. The amino acid sequences of *Cg*DBH-1 homologies from other species were downloaded from National Center for Biotechnology Information (NCBI, http://www.ncbi.nlm.gov), and used to create the multiple sequence alignment by ClustalW Multiple Alignment program (http://www.ebi.ac.uk/clustalw/). The Maximum Likelihood (ML) phylogenic tree was constructed based on the deduced amino acid sequences of DBHs by utilizing Mega 6.06 software and the reliability of the branching was tested using bootstrap of 1000.

**Table 2**
Primers used in this study.

| Primer name | Sequence (5′-3′) |
|---|---|
| ***Clone primers*** | |
| P1 (oligo dT-adaptor) | GGCCACGCGTCGACTAGTACT |
| P2 (*Cg*DBH-1-forward) | ATGGAAATGAGAACTAGTGTAATTTGC |
| P3 (*Cg*DBH-1-reverse) | GAACATAATGGTTACAAAGAAATACATAGTAT |
| ***Sequence primers*** | |
| P4 (M13-47) | CGCCAGGGTTTTCCCAGTCACGAC |
| P5 (RV-M) | GAGCGGATAACAATTTCACACAGG |
| P6 (T7-F) | TAATACGACTCACTATAGGG |
| P7 (T7-R) | TGCTAGTTATTGCTCAGCGG |
| ***RT primers*** | |
| P8 (*Cg*DBH-1-RT-forward) | TCCTTTCAATGCCAGGCTCTTCG |
| P9 (*Cg*DBH-1-RT-reverse) | ATGCTGGGGCTCCGTTGTAGATA |
| P10 (*Cg*EF-RT-forward) | AGTCACCAAGGCTGCACAGAAAG |
| P11 (*Cg*EF-RT-reverse) | TCCGACGTATTTCTTTGCGATGT |
| ***Recombination primers*** | |
| P12 (*Cg*DBH-1-Exp-22b-forward) | CGCGAATCCGTTCTCATTTTTCGCGGAAAAAAT |
| P13 (*Cg*DBH-1-Exp-22b-reverse) | CCGCTCGAGATTGTTCGACGAATTGTCATCGTTT |

### 2.6. Quantitative real-time PCR analysis

The mRNA expression of target genes was determined by quantitative real-time PCR (RT-PCR) with ABI Quantstudio sequence detection system (Applied Biosystems). The primers used in our study were all listed in Table 2, and two specific primers, P10 and P11, were used to amplify part of elongation factor (EF) (CGI_10012474) which was chosen as an internal control in oysters. Two-step method was employed for the real-time PCR cycling program, and the reaction mixture and cycling conditions were the same as previous research (Li et al., 2016). After PCR cycle, dissociation curve was performed to confirm that only one PCR product was amplified. The $2^{-\Delta\Delta CT}$ method was used to analyze the expression level of genes (Livak and Schmittgen, 2001), and all data were given in terms of relative mRNA expression of mean ± S.D. (N = 3).

### 2.7. CgDBH-1 recombination, purification and antibody preparation

The encoding sequence except for the domains of signal peptide and transmembrane domain was amplified by using primers P12 and P13 (containing enzyme cut site of *Bam*H I and *Xho* I, respectively) (Table 2). Then the PCR fragment was digested by the restriction enzymes of *Bam*H I and *Xho* I, and further inserted into the pET-22b expression vector. The recombinant plasmid (*Cg*DBH-1-pET22b) was transformed into *Escherichia coli transetta* (DE3) (Transgen) and positive transformants were incubated in Luria-Bertani (LB) medium at 37 °C with shaking at 220 rpm. When optical density of the culture medium at 600 nm reached 0.4–0.6, isopropyl-β-D-thiogalactopyranoside (IPTG) was added into the medium at a final concentration of 0.24 g $L^{-1}$ to induce the expression of recombinant protein (designed as r*Cg*DBH-1). Meanwhile, the control protein rTRX was also induced after null pET-32a plasmid was transfected into *transetta* (DE3) strain. Subsequently, r*Cg*DBH-1 and rTRX were purified by Ni affinity chromatography and dialyzed out of urea to refold the protein. Finally, the purified r*Cg*DBH-1 protein was used to immunize 6-week old mice to acquire polyclonal antibody (anti-rCgDBH-1 antibody) as previous description (Cheng et al., 2006).

### 2.8. Western blotting analysis

For verifying the specificity of polyclonal antibody, the protein of r*Cg*DBH-1 was separated by 12% SDS-PAGE and electrophoretically transferred onto nitrocellulose membrane. Subsequently, the membranes were blocked by 5% skim milk powder solution at 37 °C for 2 h and incubated with anti-r*Cg*DBH-1 antibody (diluted 1:500) at 4 °C overnight. After thoroughly washing with TBST (2.40 g $L^{-1}$ Tris-HCl, pH 8.0, 8.80 g $L^{-1}$ NaCl and 0.05% Tween-20), the membrane was incubated with horse radish peroxidase (HRP)-conjugated anti-mouse IgG (ABclonal, diluted 1:2000) at 37 °C for 1 h. After thoroughly washing with TBST, the membrane was developed with enhanced chemiluminescent (ECL) detection reagents (Thermo scientific) and imaged by Amersham Imager 600 (GE Healthcare).

### 2.9. Immunocytochemical assay

Immunocytochemical assay was conducted according to previous report (Li et al., 2018) to analyze the distribution of endogenous *Cg*DBH-1 in oyster hemocytes. Briefly, hemolymphs were collected from sinus of six oysters and deposited onto a glass slide directly. One hour later, the supernatant was discarded and attached hemocytes were fixed with 4% paraformaldehyde (PFA) at room temperature for 15 min. After washing with PBST (PBS with 0.05% Tween-20), hemocytes were permeabilized with 0.5% Triton-100 for 5 min and blocked with 3% BSA in PBST at 37 °C for 2 h. After that, the slides were incubated with the antiserum against *Cg*DBH-1 (diluted 1: 500) at 37 °C for 2 h. Following washed with PBST, hemocytes were incubated with Alexa Fluor 488-conjugated goat anti-mouse secondary antibody (ABclonal, diluted 1:2000) at 37 °C for 1 h in dark. Finally, the hemocytes nuclei were stained with DAPI (Beyotime, diluted 1:10000) for 5 min. After washing with PBST, the slides were observed under fluorescence microscope (Axio Imager A2, Zeiss).

In order to further explore the definite localization of *Cg*DBH-1, the hemocytes on slides were co-incubated with the antiserum against *Cg*DBH-1 (diluted 1: 500) and antibody of endoplasmic reticulum (ER) marker molecule, GRP78 (Beyotime, derived from rabbit and diluted at 1: 300). After washing with PBST, hemocytes were co-incubated with Alexa Fluor 488-conjugated goat anti-mouse secondary antibody (ABclonal, diluted 1:2000) and Alexa Fluor 555-conjugated goat anti-rabbit secondary antibody (Sangon, diluted 1:1000) at 37 °C for 1 h in dark. After staining with DAPI (Beyotime, diluted 1:10000) for 5 min, the hemocytes were observed under fluorescence microscope (Axio Imager A2, Zeiss).

### 2.10. Enzyme activity determination

The enzyme activity of r*Cg*DBH-1 was determined according to previous report with little modification (Liu et al., 2018b; Nagatsu and Udenfriend, 1972). Briefly, the enzymatic reaction mixture was prepared as following: 100 μL sodium acetate buffer (1.0 mol $L^{-1}$, pH 5.0), 25 μL sodium fumarate (0.2 mol $L^{-1}$), 25 μL freshly prepared ascorbic acid (0.2 mol $L^{-1}$), 25 μL catalase (1.0 mg $mL^{-1}$), 25 μL tyramine (0.4 mol $L^{-1}$), 25 μL pargyline (20.0 mmol $L^{-1}$), and 75 μL N-ethylmaleimide (0.2 mol $L^{-1}$). After fully premixing, 50 μL (50 μmol $L^{-1}$) r*Cg*DBH-1 or rTRX was added into the mixture, respectively. The boiled protein of r*Cg*DBH-1 (95 °C for 5 min) was used as blank. The reaction mixture was incubated at 37 °C for 60 min in a water bath with continual shaking. Subsequently, the concentration of octopamine was quantified by octopamine ELISA Kit (TSZ) based on the manufacturer's instruction. Fifty microliter samples were added into a 96 micro-well plate and incubated at 37 °C for 45 min. After washing with washing buffer for four times, 50 μL biotinylated anti-IgG of octopamine and 50 μL streptavidin-HRP were respectively added and incubated in the 96 micro-well plate. Then tetramethylbenzidine (TMB) chromogenic substrate was added and incubated for 15 min at 37 °C, and the fluorescence intensity in each micro-well was measured at 450 nm (Tecan). The concentration of octopamine was determined based on standard curves, and the dopamine-β-hydroxylase activity was calculated according to the manual.

### 2.11. Statistical analysis

All data were presented as mean ± S.D., and analyzed by statistical package for social sciences (SPSS) 16.0. Statistical differences between samples were tested using ANOVA (Duncan's test), and differences were considered statistically significant at $p < 0.05$ and extremely significant at $p < 0.01$.

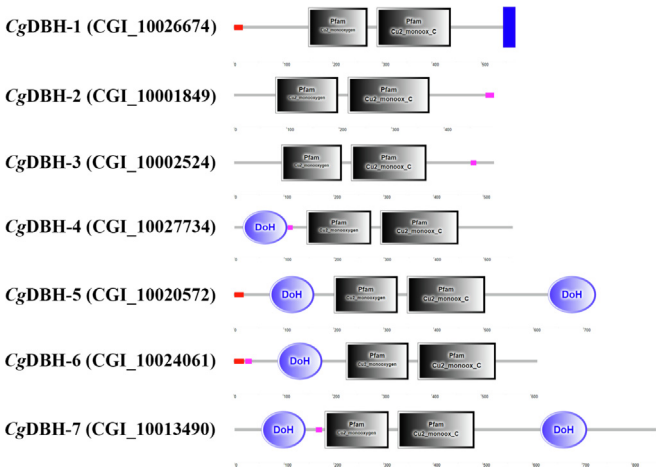


**Fig. 1.** The protein domain structure of DBH family members screened from oyster *C. gigas* genome. The oyster genome with gene annotation was conducted to screen members of dopamine β-hydroxylase (DBH) family. Seven members (*Cg*DBH-1～*Cg*DBH-7) were identified and their amino acid sequences were retrieved from OysterBase, which were further used for prediction of protein domains by SMART version 8.0. The conserved Cu2_monooxygen domain and DoH (DOMON) domain were identified, and a transmembrane domain was also predicted in *Cg*DBH-1.

## 3. Results

### 3.1. The DBH family screened from oyster genome

According to the oyster genome information (Zhang et al., 2012), seven DBH genes with varied molecular mass were screened and their basic information were shown in Table 1. The protein domain analysis revealed that, all members contained two conserved Cu2_monooxygen domains. There were one or two additional DoH (DOMON) domain identified in *Cg*DBH-4～*Cg*DBH-7 (Fig. 1). Among the seven DBHs, only *Cg*DBH-1 was identified to contain a transmembrane domain.

The expression pattern of the seven DBHs was analyzed according to the transcription data released by Zhang (Zhang et al., 2012), and a tissue specific expression pattern was validated (Fig. 2). Among the seven members, *Cg*DBH-1 was shown to be dominantly expressed in hemocytes (Hem), while *Cg*DBH-2 was overwhelmingly expressed in gills (Gil) and labial palp (Lpa), and *Cg*DBH-7 was mainly expressed in digestive gland (Dgl) (Fig. 2). By comparison, *Cg*DBH-3 and *Cg*DBH-5 was moderately expressed in mantle (MO and MI) and digestive gland, respectively. The transcripts of *Cg*DBH-4 and *Cg*DBH-6 were hardly undetectable in these adult tissues. To further explore the possible regulatory role of DBH in immune response, the *Cg*DBH-1, which was highly expressed in hemocytes, was cloned for further research.

### 3.2. The sequence characters and phylogeny relationship of CgDBH-1

The coding sequence of *Cg*DBH-1 was amplified with primers P2 and P3, which was of 1707 bp encoding a protein with 568 amino acids. The molecular mass of *Cg*DBH-1 was predicted to be 64.7 kDa with a theoretical isoelectric point of 5.56. SMART analysis revealed that *Cg*DBH-1 contained an N-terminal signal peptide ($Met_1$-$Gly_{19}$), two $Cu_H$ and $Cu_M$ domains ($Asn_{151}$-$Ser_{270}$ and $Ala_{289}$-$Phe_{438}$) and a C-terminal transmembrane domain ($Gly_{545}$-$Met_{567}$). The deduced amino acid sequence of *Cg*DBH-1 shared 30.1% similarity with DBH from *Mus musculus* (NP_620392), and 30.9% with that of *Homo sapiens* (NP_000778). Nine conserved cysteine residues were identified in *Cg*DBH-1 by multiple alignment (Fig. 3). The conserved cysteine residues were marked with blue filled triangles. The active sites of $Cu_H$ ($His_{197}$, $His_{198}$ and $His_{262}$) and $Cu_M$ ($His_{333}$, $His_{335}$ and $Met_{408}$) domain were indicated with red balls and red filled triangles, respectively.

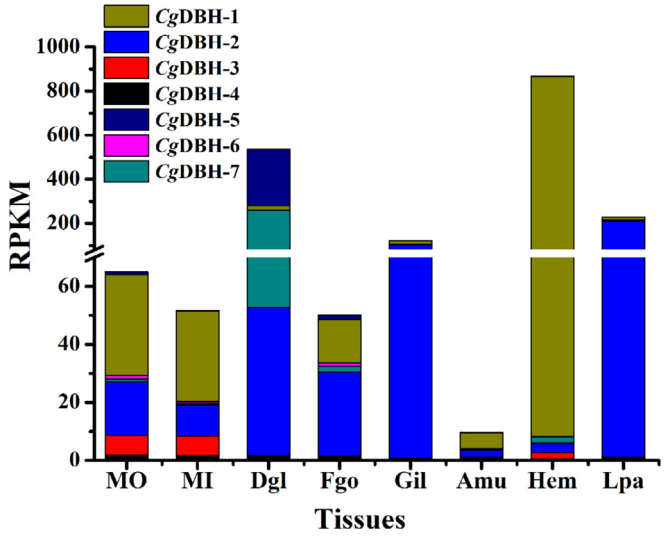


**Fig. 2.** The varied expression level of *Cg*DBH members in different tissues of adult oysters. The expression level of each gene was expressed as RPKM (Reads Per Kilobase per Million mapped reads) value, of which the data were retrieved from previous transcriptomic data of oyster (Zhang et al., 2012). MO, outer edge of mantle; MI, inner pallial part of mantle; Dgl, digestive gland; Fgo, female gonad; Gil, gills; Amu, adductor muscle; Hem, hemocytes; Lap, labial palp.

A phylogenetic tree was constructed to analyze the molecular evolutionary relationship of *Cg*DBH-1 with DBHs from other species by using Maximum Likelihood (ML) method. Those DBHs were distinctly separated into two major groups: vertebrate branch and invertebrate branch. The *Cg*DBH-1 was closely clustered with DBH from mollusk *Aplysia californica*, and then joined into the invertebrates group (Fig. 4).

### 3.3. The recombinant protein and polyclonal antibody of CgDBH-1

The recombinant plasmid (*Cg*DBH-pET22b) was constructed and transformed into *E. coli transetta* (DE3) to prokaryotically express r*Cg*DBH-1. The whole cell lysate of positive clone strain after IPTG induction was analyzed by SDS-PAGE. A distinct band with a molecular mass of nearly 64.0 kDa was revealed as predicted (Fig. 5). The purified r*Cg*DBH-1 protein was used to obtain polyclonal antibody. The antibody specificity was tested by western blotting and a clear band was revealed (Fig. 5).

### 3.4. The enzyme activity of rCgDBH-1 protein

The enzyme activity of r*Cg*DBH-1 protein was estimated by the production of octopamine and calculated based on the standard curve. The enzyme activity of r*Cg*DBH-1 protein was 0.54 ± 0.019 pmol $L^{-1}$ $min^{-1}$ and it was significantly higher ($p < 0.01$) than that in rTRX group (0.098 ± 0.034 pmol $L^{-1}$ $min^{-1}$) and blank group where the enzyme activity of DBH was nearly undetectable (Fig. 6).

### 3.5. The validation of CgDBH-1 expression pattern in various tissues and three subtypes of hemocytes

Quantitative real-time PCR was employed to validate the mRNA expression of *Cg*DBH-1 in different tissues of oyster, including hepatopancreas, mantle, gonad, adductor muscle, gills, hemocytes, labial palp and visceral ganglia. The highest expression level of *Cg*DBH-1 transcript was detected in hemocytes, which was 90.48 ± 41.87 fold ($p < 0.01$) of that in gonad (Fig. 7). *Cg*DBH-1 was also highly expressed in visceral ganglia and hepatopancreas, which was 35.76 ± 20.37 fold and 18.89 ± 2.30 fold ($p < 0.01$) of that in gonad, respectively (Fig. 7). There was no significant difference on the mRNA expression of *Cg*DBH-1 among the rest tissues, including mantle, gonad, adductor muscle, gills and labial palp (Fig. 7).

The mRNA expressions of *Cg*DBH-1 were also examined in the separated hemocytes of three subtypes. The expressions of *Cg*DBH-1 in granulocytes and semi-granulocytes were significantly higher than the average level in the total hemocytes (Fig. 8), which was 3.93 ± 0.28 fold ($p < 0.01$) and 2.16 ± 0.37 fold ($p < 0.01$) of that in the total hemocytes, respectively. The mRNA expression of *Cg*DBH-1 was lowest in agranulocytes, compared with that in other cell sub-populations, which was 0.48 ± 0.03 fold ($p < 0.01$) of that in the total hemocytes (Fig. 8).

### 3.6. The subcellular distribution of CgDBH-1 protein in oyster hemocytes

Immunofluorescence assay was conducted to explore the expression pattern of *Cg*DBH-1 in hemocytes of three subtypes and its subcellular localization in hemocytes. The positive signal of *Cg*DBH-1 protein was observed in green, which was mainly distributed in some (not all) granulocytes, while no positive signal was detected in semi-

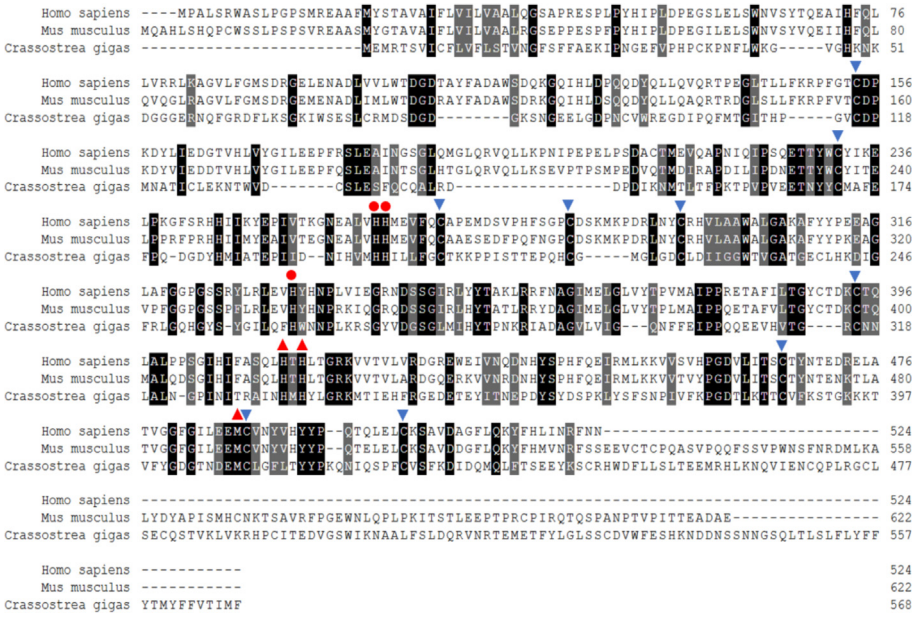


**Fig. 3.** Multiple sequence alignment analysis of *Cg*DBH-1 with DBHs from *Homo sapiens* and *Mus musculus*. The amino acid sequences of DBHs from *Homo sapiens* (NP_000778) and *Mus musculus* (NP_620392) were retrieved from GenBank. These sequences together with that of *Cg*DBH-1 were used for multiple sequence alignment analysis. The identical amino acid residues were shaded in black and the similar amino acid were shaded in grey. The conserved cysteine residues were marked with blue filled triangles. The active sites of $Cu_H$ ($His_{197}$, $His_{198}$ and $His_{262}$) and $Cu_M$ ($His_{333}$, $His_{335}$ and $Met_{408}$) domain were identified and indicated with red balls and red filled triangles, respectively.

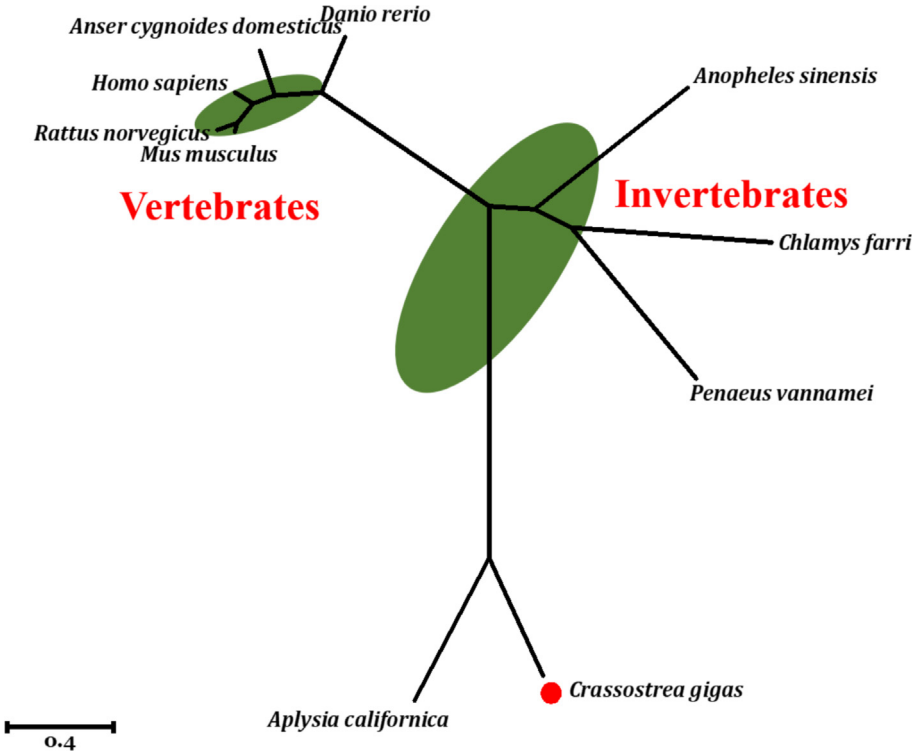


**Fig. 4.** Maximum likelihood (ML) phylogeny tree based on the amino acid sequences of different DBHs. The DBHs from different organisms used for phylogenetic analysis include: *Homo sapiens* (NP_000778), *Mus musculus* (NP_620392), *Danio rerio* (AAI63055), *Rattus norvegicus* (AAA41091), *Anopheles sinensis* (KFB49424), *Penaeus vannamei* (ANA78437), *Anser cygnoides domesticus* (AMN15063), *Aplysia californica* (NP_001191657) and *Azumapecten farreri* (ADP08787). Their amino acid sequences retrieved from GenBank were used for construction of phylogeny tree by using Maximum Likelihood (ML) method. The *Cg*DBH-1 was closely clustered with DBH from mollusk *Aplysia californica*, and joined into the invertebrate group. The scale bar represented conversion of branch length to genetic distance between clades.

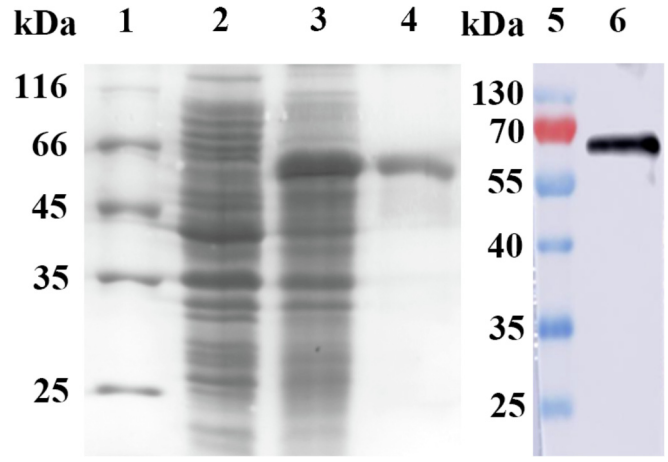


**Fig. 5.** SDS-PAGE and western-blot analysis of r*Cg*DBH-1. The recombinant plasmid containing encoding sequence of *Cg*DBH-1 was transformed into *Escherichia coli transetta* (DE3). r*Cg*DBH-1 was prokaryotically expressed in *transetta* (DE3) and purified by Ni affinity chromatography, which was further used for preparing the polyclonal antibody against r*Cg*DBH-1. The whole proteins of *transetta* (DE3) before and after induction were analyzed by SDS-PAGE, and the specificity of prepared antibody was validated by western-blot. The distinct band of r*Cg*DBH-1 was revealed in *transetta* (DE3) after induction, and a specific band was shown by prepared polyclonal antibody. Lane 1 and 5: protein molecular standard; Lane 2: negative control for *transetta* (DE3) without induction; Lane 3: whole protein of *transetta* (DE3) with induction; Lane 4: purified r*Cg*DBH-1; Lane 6: western-blot based on the sample of lane 4 with prepared polyclonal antibody against r*Cg*DBH-1.

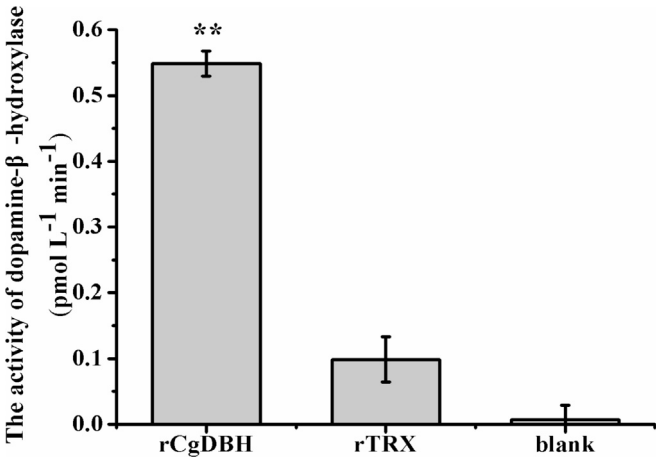


**Fig. 6.** The enzyme activity of recombinant *Cg*DBH-1 protein. The enzyme activity was validated by production of NE, and the amount of product was calculated based on standard curve. The boil-inactivated r*Cg*DBH-1 protein was regarded as blank and rTRX protein was used as control. Significant enzyme activity of r*Cg*DBH-1 was detected. Vertical bars represented the mean ± S.D. and asterisks indicated extremely significant differences ($p < 0.01$, ANOVA).

granulocytes or agranulocytes (Fig. 9A). The green signal of *Cg*DBH-1 protein was distributed in the cytoplasm and partly co-localized with granules of granulocytes (Fig. 9A). After the ER was labeled with antibody of marker protein GRP78 (red), the positive signal of endogenous *Cg*DBH-1 protein (green) was also co-localized with ER in oyster hemocytes (Fig. 9B).

### 3.7. The temporal mRNA expression of *CgDBH-1* after LPS stimulation

The dynamic mRNA expression of *Cg*DBH-1 in oyster hemocytes post LPS stimulation was detected by quantitative real-time PCR. The expression level of *Cg*DBH-1 was up-regulated significantly at 24 and 48 h after LPS stimulation, which was about 2.99-fold ($p < 0.01$) and 2.56-fold ($p < 0.01$) of that in PBS group, respectively (Fig. 10). And there was no significant expression difference of *Cg*DBH-1 transcript between the PBS and LPS group at 0, 3, 6, 12, 72 and 96 h post stimulation (Fig. 10).

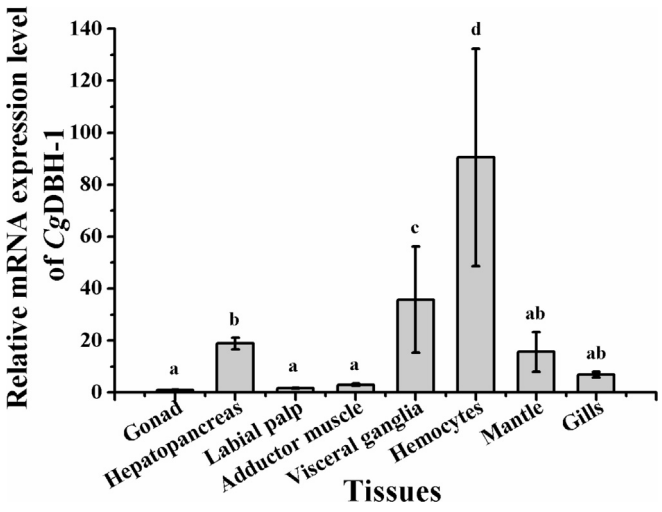


**Fig. 7.** The mRNA expression level of *Cg*DBH-1 in different tissues of adult oysters. The mRNA expression level was detected by RT-PCR and *Cg*DBH-1 was significantly high expressed in hemocytes. Data were represented as the ratio of the *Cg*DBH-1 mRNA level to that of EF and normalized to that of in gonad. Vertical bars represented the mean ± S.D. (N = 3) and the letters (a, b, c and d) indicated extremely significant differences ($p < 0.01$, ANOVA).

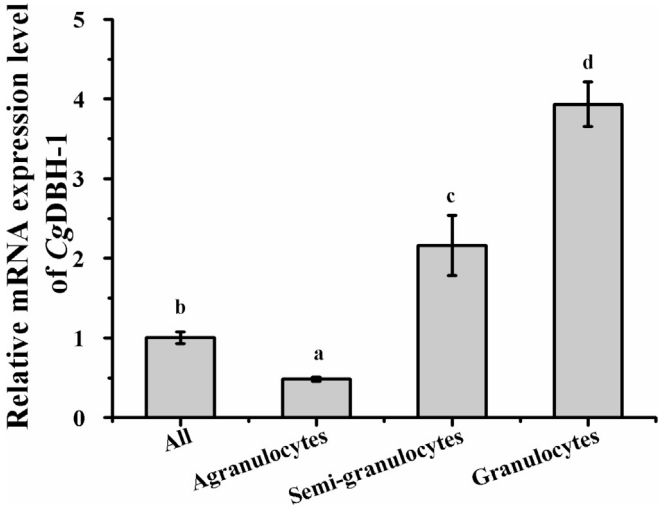


**Fig. 8.** The mRNA expression level of *Cg*DBH-1 in different subtypes of hemocytes. The three subtypes of hemocytes (granulocytes, semi-granulocytes and agranulocytes) were separated and used for detection the expression level of *Cg*DBH-1. *Cg*DBH-1 was significant highly expressed in granulocytes. Data were represented as the ratio of the *Cg*DBH-1 mRNA level to that of EF and normalized to that of total hemocytes. Vertical bars represented the mean ± S.D. (N = 3) and the letters (a, b, c and d) indicated extremely significant differences ($p < 0.01$, ANOVA).

## 4. Discussions

Functional interactions between the neuroendocrine and immune systems are well-identified in both vertebrate and invertebrate animals (Demas et al., 2011; Kawli et al., 2010). In vertebrates, the neuroendocrine and immune systems are mainly linked by two primary pathways: (i) the sympathoadrenal system (SAS), via either direct neural innervation of lymphoid tissue or CAs release from the adrenal medulla and (ii) the hypothalamo-pituitary-adrenal (HPA) axis and subsequent release of glucocorticoids from the adrenal cortex (Demas et al., 2011; Padgett and Glaser, 2003). However, in invertebrates, the neuroendocrine system is far more primitive than that of vertebrates, and most invertebrates own open circulatory system without blood brain barrier, such as bivalve oyster *C. gigas* (Bourne et al., 1990; Bundgaard and Abbott, 1992). Therefore, the circulatory immune cells, which could synthesize and secret neurotransmitters, might play an extremely important role for hemostasis maintaining, and might be a vital breakthrough point to explore the functional integrity of NEI network in invertebrates.

CAs have often been regarded as immunosuppressive hormones or transmitters (Elenkov et al., 2000), and could be synthesized in lymphocytes and phagocytes in vertebrates to participate in immune regulation via an autocrine loop (Bergquist et al., 1994; Flierl et al., 2007). DBH is an important rate-limiting enzyme involved in the synthesis of CAs by catalyzing the conversion of DA to NE (Scanzano and Cosentino, 2015). The expressions of DBH have been identified in macrophages and neutrophils from rats (Bergquist et al., 1994; Flierl et al., 2007). The DBH activity was also detectable in hemocytes of invertebrates, such as oysters (Liu et al., 2018b). In order to identify the molecular basis for NE synthesizing in oyster hemocytes, the DBH gene family was analyzed after screening from the genome of oyster *C. gigas*. Total of seven DBH family members with varied molecular mass were identified in oyster genome, and they all possessed two conserved $Cu_H$ and $Cu_M$ domains. The $Cu_H$ and $Cu_M$ domains were the most important functional domain of DBH family and responsible for their enzymatic activities (Torres Pazmiño et al., 2010). Except for the conserved $Cu_H$ and $Cu_M$ domains, one or two additional DoH (DOMON) domains were identified in *Cg*DBH-4–7. DoH domain was a possible catecholamine-binding domain present in a variety of eukaryotic proteins, whose function remains unknown at present (Vendelboe et al., 2016). As DoH domain was not present in all DBH members, it might not be an indispensable functional domain in DBH family. Different from other DBHs in oyster, a transmembrane domain was predicted in C-terminal of *Cg*DBH-1. The DBHs in vertebrates were reported to exist in soluble or membrane-bound form, which were encoded by the same gene (Lewis and Asnani, 1992). The presence of transmembrane domain in *Cg*DBH-1 suggested that it might exist as a membrane-bound form in oyster. It was suspected that there were other DBH members without transmembrane domain might function as soluble form in oyster. The two forms of DBHs were encoded by different genes in oysters, which was quite different from that in vertebrates. These results collectively suggested that *Cg*DBH-1 was a novel membrane-bound form DBH in mollusk. Moreover, a tissue specific expression pattern of *Cg*DBH members in adult tissues was validated in the present study, possibly indicating the functional differentiations within members of DBH family in oyster. Among them, *Cg*DBH-1 was dominantly high expressed in hemocytes, which was far more richness than other members. All these results gave a clue that *Cg*DBH-1 was a hemocyte-specific type of DBH in oysters, which was chosen for further investigating the neurotransmitters derived from immunocytes and their modulation function in the immune response.

The molecular characteristics of *Cg*DBH-1 were explored by multiple alignment analysis. The deduced amino acid sequence of *Cg*DBH-1 shared 30.1% and 30.9% similarity with that of *M. musculus* and *H. sapiens*, respectively. The conserved cysteine residues in $Cu_H$ ($His_{197}$, $His_{198}$ and $His_{262}$) and $Cu_M$ ($His_{333}$, $His_{335}$ and $Met_{408}$) domain were also identified in *Cg*DBH-1, which were inferred to be important for the catalytic activity of DBH. *Cg*DBH-1 was closely clustered with DBH from *Aplysia californica* in the phylogenetic tree, and then joined in the group of invertebrates. Those results collectively suggested that *Cg*DBH-1 might be a homologue of DBH family in mollusk. To validate the physical function of *Cg*DBH-1, the recombinant *Cg*DBH-1-pET22b was prokaryotically expressed, and r*Cg*DBH-1 could promote the production of NE, indicating that r*Cg*DBH-1 possessed the catalytic activity of DBH family. These results confirmed that the *Cg*DBH-1 was a member of DBH family with the activity to synthesize NE.

Generally, DBH was mostly distributed in chromaffin cells and adrenergic neurons of vertebrates (Oyarce and Eipper, 2000). To validate the distribution of *Cg*DBH-1 in oyster, its expression pattern in

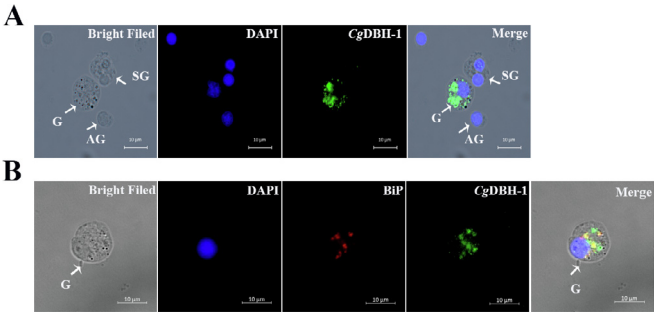


**Fig. 9.** The subcellular distribution of *Cg*DBH-1 in oyster hemocytes detected by fluorescence microscope. (A) The nuclei of hemocytes were strained with DAPI (blue) and the positive signal of *Cg*DBH-1 was visualized by Alexa Fluor 488-conjugated goat anti-mouse IgG (green). The *Cg*DBH-1 protein was mainly detected in granulocytes. (B) The nuclei of hemocytes were strained with DAPI (blue) and the positive signal of *Cg*DBH-1 was visualized by Alexa Fluor 488-conjugated goat anti-mouse IgG (green). The ER marker molecule GRP78 was visualized by Alexa Fluor 555-conjugated goat anti-rabbit (red) and the positive signal of *Cg*DBH-1 overlapped with ER marker molecule GRP78 was in yellow. The *Cg*DBH-1 protein was mainly detected to be co-located with ER in granulocytes.

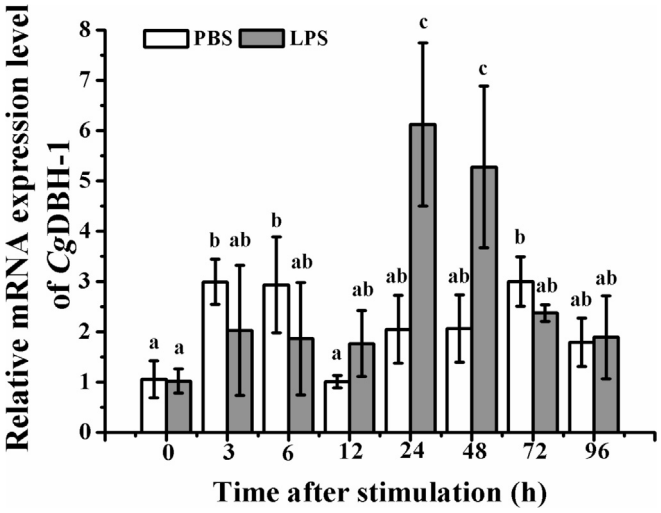


**Fig. 10.** Temporal mRNA expression change of *Cg*DBH-1 in oyster hemocytes after LPS stimulation. The expression levels of *Cg*DBH-1 in hemocytes were monitored at 0, 3, 6, 12, 24, 48, 72 and 96 h after LPS stimulation, with PBS stimulation group as control. *Cg*DBH-1 was significantly induced in hemocytes at 48 and 72 h after LPS stimulation. Data were represented as the ratio of the *Cg*DBH-1 mRNA level to that of EF and normalized to 0 h. Vertical bars represent the mean ± S.D. (N = 3) and the letters (a, b and c) indicated extremely significant differences ($p < 0.01$, ANOVA).

adult tissues was monitored in the present study, and similar expression pattern was also detected. *Cg*DBH-1 was higher expressed in visceral ganglia and hepatopancreas, compared with that in tissues of gonad, labial palp, adductor muscle, mantle and gills. Interestingly, as indicated in the genomic data, *Cg*DBH-1 was detected to be highest expressed in oyster hemocytes, which was even 2.53-fold of that in visceral ganglia. Circulating hemocytes are the main immunocytes in mollusk which play a major role in immune defense and homeostasis maintaining (Wang et al., 2013). In oysters, the hemocytes derived NE was reported to regulate immune response after LPS stimulation (Liu et al., 2018b). In vertebrates, DBH was also reported to be expressed in the specific types of immunocytes and could mediate the production of NE which played important roles in immune regulation (Bergquist et al., 1994; Flierl et al., 2007). The circulating hemocytes of oysters were mainly classified into three types: granulocytes, semi-granulocytes and agranulocytes (Wang et al., 2017). *Cg*DBH-1 transcript could be detected in all kinds of hemocytes with highest expression level in granulocytes. Granulocytes in oysters were demonstrated to be the main cell-type functioning in phagocytosis and production of cytokines (Wang et al., 2017). The surprisingly high expression level of *Cg*DBH-1 in granulocytes suggested that *Cg*DBH-1 might be involved in the immune regulation of phagocytosis and inflammation, which was similar with phagocytes-specific DBH in mice (Flierl et al., 2007). The subcellular localization of *Cg*DBH-1 protein in oyster hemocytes was further confirmed that the transmembrane *Cg*DBH-1 protein was mainly located in the cytoplasm of granulocyte and co-localized with granules and ER. In vertebrates' chromaffin cells at resting state, there are two isoforms of DBH protein encoded by same gene, the membrane and the soluble DBH, which are located in secretory granules (catecholamine-containing organelles) membrane and within granules, respectively (Markoglou and Wainer, 2001; Wick et al., 1997). After chromaffin cells are activated, the membrane of granules is fused with cytomembrane, and the soluble DBH inside granules is secreted and functions in hemolymph. Then the cytomembrane-fused membrane DBH is recycled, transported back and fused with fresh granules membrane, and further functions in hemocytes (Wick et al., 1997). Therefore, the DBH in vertebrates could exist as membrane and soluble form and work in both hemolymph and hemocytes. While in oysters, there were seven DBH family members annotated in oyster genome and only *Cg*DBH-1 had a transmembrane domain. As *Cg*DBH-1 protein was mainly distributed in the cytoplasm of oyster hemocytes, it was inferred that the transmembrane *Cg*DBH-1 functioned in oyster hemocytes. It was suspected that there was other soluble DBHs encoded by other genes working in hemolymph. *Cg*DBH-1 protein was co-localized with ER of oyster hemocytes, indicating that it was a secretory membrane protein to be processed and matured in ER (Hurtley, 1993). The result was consistent with the subcellular localizations of vertebrates' DBH when they were expressed in AtT-20 corticotrope tumor cells and Chinese hamster ovary cells (Oyarce and Eipper, 2000; Xin et al., 2004).

DBH was reported to participate in immune response and could be significantly induced after immune stimulation to promote the production of NE. In mice, the DBH in phagocytes could be un-regulated by LPS stimulation (Flierl et al., 2007). In the present study, the expressions of *Cg*DBH-1 in hemocytes after LPS stimulation were significantly increased at 24 h and 48 h, which was consistent with dynamic change of NE in hemolymph supernatant of oysters after LPS stimulation (Liu et al., 2017). These results indicated that *Cg*DBH-1 could respond to immune stimulation and might function at the late phase of immune response in oysters. Recently, NE was reported to execute a negative regulation on hemocyte phagocytosis and synthesis of immune effectors in oysters (Liu et al., 2018b). The highly expressed *Cg*DBH-1 in the late phase of immune reaction could promote the production of NE, which could down-regulate immune response and avoid over reaction. Therefore, all those results implied that NE could be synthesized by *Cg*DBH-1 in oyster granulocytes and execute immunosuppressive function at the late phase of immune stimulation to avoid excessive immune response.

In conclusion, one novel DBH with a transmembrane domain was identified in oysters, and it possessed the enzymatic activity for synthesizing NE. The mRNA of *Cg*DBH-1 was highly expressed in the hemocytes, especially in the granulocytes of oysters. Moreover, the *Cg*DBH-1 protein was mainly co-localized with the granules and endoplasmic reticulum (ER) of granulocytes. The expression of *Cg*DBH-1 in hemocytes was significant increased at the late stage of immune stimulation. Those results collectively suggested that, *Cg*DBH-1, as a novel invertebrate NE synthesizing enzyme, was highly expressed in granulocytes and involved in immune response of oysters, which provided a novel insight to understand the crosstalk between neuroendocrine and immune systems in invertebrates.

## Acknowledgements

We are grateful to all the laboratory members for their technical advice and helpful discussions. This research was supported by grants from National Science Foundation of China (No. U1706204), National Key R&D Program (2018YFD0900606), earmarked fund (CARS-49) from Modern Agro-industry Technology Research System, the Fund for Outstanding Talents and Innovative Team of Agricultural Scientific Research, the AoShan Talents Cultivation Program Supported by Qingdao National Laboratory for Marine Science and Technology (No. 2017ASTCP-OS13), the Distinguished Professor of Liaoning (to L. S.), Key R&D Program of Liaoning Province (2017203001 to L.W.), and Natural Science Foundation of Liaoning, China (20170520056), Dalian High Level Talent Innovation Support Program (2015R020), and Talented Scholars in Dalian Ocean University.

## References

Alaniz, R.C., Thomas, S.A., Perez-Melgosa, M., Mueller, K., Farr, A.G., Palmiter, R.D., Wilson, C.B., 1999. Dopamine β-hydroxylase deficiency impairs cellular immunity. Proc. Natl. Acad. Sci. U.S.A. 96, 2274–2278.

Bergquist, J., Tarkowski, A., Ekman, R., Ewing, A., 1994. Discovery of endogenous catecholamines in lymphocytes and evidence for catecholamine regulation of lymphocyte function via an autocrine loop. Proc. Natl. Acad. Sci. U.S.A. 91, 12912–12916.

Bourne, G.B., Redmond, J.R., Jorgensen, D.D., 1990. Dynamics of the molluscan circulatory system: open versus closed. Physiol. Zool. 63, 140–166.

Bundgaard, M., Abbott, N.J., 1992. Fine structure of the blood-brain interface in the cuttlefish *Sepia officinalis* (Mollusca, Cephalopoda). J. Neurocytol. 21, 260–275.

Cheng, S., Zhan, W., Xing, J., Sheng, X., 2006. Development and characterization of monoclonal antibody to the lymphocystis disease virus of Japanese flounder *Paralichthys olivaceus* isolated from China. J. Virol Methods 135, 173–180.

Cheng, W., Ka, Y.W., Chang, C.C., 2017. Involvement of dopamine β-hydroxylase in the neuroendocrine-immune regulatory network of white shrimp, *Litopenaeus vannamei*. Fish Shellfish Immunol. 68, 92–101.

Demas, G.E., Adamo, S.A., French, S.S., 2011. Neuroendocrine-immune crosstalk in vertebrates and invertebrates: implications for host defence. Funct. Ecol. 25, 29–39.

Elenkov, I.J., Wilder, R.L., Chrousos, G.P., Vizi, E.S., 2000. The Sympathetic Nerve-An integrative interface between two supersystems: the brain and the immune system. Pharmacol. Rev. 52, 595–638.

Evans, O., Hick, P., Whittington, R.J., 2017. Detection of *Ostreid herpesvirus-1* microvariants in healthy *Crassostrea gigas* following disease events and their possible role as reservoirs of infection. J. Invertebr. Pathol. 148, 20–33.

Flierl, M.A., Rittirsch, D., Nadeau, B.A., Chen, A.J., Sarma, J.V., Zetoune, F.S., et al., 2007. Phagocyte-derived catecholamines enhance acute inflammatory injury. Nature 449, 721–U728.

Fujii, T., Mashimo, M., Moriwaki, Y., Misawa, H., Ono, S., Horiguchi, K., Kawashima, K., 2017. Expression and function of the cholinergic system in immune cells. Front. Immunol. 8, 1085.

Hurtley, S.M., 1993. Recycling of a secretory granule membrane protein after stimulated secretion. J. Cell Sci. 106, 649–656.

Kawli, T., He, F., Tan, M.W., 2010. It takes nerves to fight infections: insights on neuro-immune interactions from *C. elegans*. Dis. Model. Mech. 3, 721–731.

Kimura, Y., Yoshida, M., Morisawa, M., 2003. Interaction between noradrenaline or adrenaline and the β1-adrenergic receptor in the nervous system triggers early metamorphosis of larvae in the ascidian, *Ciona savignyi*. Dev. Biol. 258, 129–140.

Kvetňanský, R., Sabban, E.L., Palkovits, M., 2009. Catecholaminergic systems in stress: structural and molecular genetic approaches. Physiol. Rev. 89, 535–606.

Lacoste, A., Jalabert, F., Malham, S.K., Cueff, A., Poulet, S.A., 2001. Stress and stress-induced neuroendocrine changes increase the susceptibility of juvenile oysters (*Crassostrea gigas*) to *Vibrio splendidus*. Appl. Environ. Microbiol. 67, 2304–2309.

Lewis, E.J., Asnani, L.P., 1992. Soluble and membrane-bound forms of dopamine β-hydroxylase are encoded by the same mRNA. J. Biol. Chem. 267, 494–500.

Li, M., Qiu, L., Wang, L., Wang, W., Xin, L., Li, Y., Liu, Z., Song, L., 2016. The inhibitory role of gamma-aminobutyric acid (GABA) on immunomodulation of Pacific oyster *Crassostrea gigas*. Fish Shellfish Immunol. 52, 16–22.

Li, H., Yin, B., Wang, S., Fu, Q., Xiao, B., Lu, K., He, J., Li, C., 2018. RNAi screening identifies a new Toll from shrimp *Litopenaeus vannamei* that restricts WSSV infection through activating Dorsal to induce antimicrobial peptides. PLoS Pathog. 14, e1007109.

Liu, Z., Zhou, Z., Jiang, Q., Wang, L., Yi, Q., Qiu, L., Song, L., 2017. The neuroendocrine immunomodulatory axis-like pathway mediated by circulating haemocytes in pacific oyster *Crassostrea gigas*. Open Biol. 7, 160289.

Liu, Z., Li, M., Yi, Q., Wang, L., Song, L., 2018a. The neuroendocrine-immune regulation in response to environmental stress in marine bivalves. Front. Physiol. 9, 1456.

Liu, Z., Wang, L., Lv, Z., Zhou, Z., Wang, W., Li, M., Yi, Q., Qiu, L., Song, L., 2018b. The cholinergic and adrenergic autocrine signaling pathway mediates immunomodulation in oyster *Crassostrea gigas*. Front. Immunol. 9, 284.

Livak, K.J., Schmittgen, T.D., 2001. Analysis of relative gene expression data using real-time quantitative PCR and the $2^{-\Delta\Delta CT}$ method. Methods 25 (4), 402–408.

Malagoli, D., Ottaviani, E., 2017. Cross-talk among immune and neuroendocrine systems in molluscs and other invertebrate models. Horm. Behav. 88, 41–44.

Markoglou, N., Wainer, I.W., 2001. Synthesis and characterization of immobilized dopamine β-hydroxylase in membrane-bound and solubilized formats. J. Biochem. Biophys. Methods 48 (1), 61–75.

Nagatsu, T., Udenfriend, S., 1972. Photometric assay of dopamine-β-hydroxylase activity in human blood. Clin. Chem. 18, 980–983.

Oyarce, A.M., Eipper, B.A., 2000. Cell type-specific storage of dopamine β-monooxygenase. J. Biol. Chem. 275, 3270–3278.

Padgett, D.A., Glaser, R., 2003. How stress influences the immune response. Trends Immunol. 24, 444–448.

Raison, C.L., Capuron, L., Miller, A.H., 2006. Cytokines sing the blues: inflammation and the pathogenesis of depression. Trends Immunol. 27, 24–31.

Reardon, C., Murray, K., Lomax, A.E., 2018. Neuroimmune communication in health and disease. Physiol. Rev. 98, 2287–2316.

Sabban, E.L., Kvetňanský, R., 2001. Stress-triggered activation of gene expression in catecholaminergic systems: dynamics of transcriptional events. Trends Neurosci. 24, 91–98.

Scanzano, A., Cosentino, M., 2015. Adrenergic regulation of innate immunity: a review. Front. Pharmacol. 6, 171.

Srivastava, M., Begovic, E., Chapman, J., Putnam, N.H., Hellsten, U., Kawashima, T., et al., 2008. The *Trichoplax* genome and the nature of placozoans. Nature 454, 955–960.

Tang, S., Yao, B., Li, N., Lin, S., Huang, Z., 2018. Association of dopamine β-hydroxylase polymorphisms with Alzheimer's Disease, Parkinson's Disease and Schizophrenia: evidence based on currently available loci. Cell. Physiol. Biochem. 51, 411–428.

Torres Pazmiño, D.E., Winkler, M., Glieder, A., Fraaije, M.W., 2010. Monooxygenases as biocatalysts: classification, mechanistic aspects and biotechnological applications. J. Biotechnol. 146, 9–24.

Trillo, L., Das, D., Hsieh, W., Medina, B., Moghadam, S., Lin, B., Dang, V., Sanchez, M.M., De Miguel, Z., Ashford, J.W., Salehi, A., 2013. Ascending monoaminergic systems alterations in Alzheimer's disease. Translating basic science into clinical care. Neurosci. Biobehav. Rev. 37, 1363–1379.

Vendelboe, T.V., Harris, P., Zhao, Y., Walter, T.S., Harlos, K., El Omari, K., Christensen, H.E.M., 2016. The crystal structure of human dopamine β-hydroxylase at 2.9 Å resolution. Science 2, e1500980.

Verburg-van Kemenade, B.M.L., Cohen, N., Chadzinska, M., 2017. Neuroendocrine-immune interaction: evolutionarily conserved mechanisms that maintain allostasis in an ever-changing environment. Dev. Comp. Immunol. 66, 2–23.

Wang, L., Qiu, L., Zhou, Z., Song, L., 2013. Research progress on the mollusc immunity in China. Dev. Comp. Immunol. 39 (1–2), 2–10.

Wang, W., Li, M., Wang, L., Chen, H., Liu, Z., Jia, Z., Qiu, L., Song, L., 2017. The granulocytes are the main immunocompetent hemocytes in *Crassostrea gigas*. Dev. Comp. Immunol. 67, 221–228.

Westfall, J.A., Elliott, S.R., MohanKumar, P.S., Carlin, R.W., 2000. Immunocytochemical evidence for biogenic amines and immunogold labeling of serotonergic synapses in tentacles of *Aiptasia pallida* (Cnidaria, Anthozoa). Invertebr. Biol. 119, 370–378.

Wick, P.F., Trenkle, J.M., Holz, R.W., 1997. Punctate appearance of dopamine-β-hydroxylase on the chromaffin cell surface reflects the fusion of individual chromaffin granules upon exocytosis. Neuroscience 80 (3), 847–860.

Xin, X., Mains, R.E., Eipper, B.A., 2004. Monooxygenase X, a member of the copper-dependent monooxygenase family localized to the endoplasmic reticulum. J. Biol. Chem. 279, 48159–48167.

Zhang, G., Fang, X., Guo, X., Li, L., Luo, R., Xu, F., et al., 2012. The oyster genome reveals stress adaptation and complexity of shell formation. Nature 490, 49–54.

Zhang, G., Li, L., Meng, J., Qi, H., Qu, T., Xu, F., Zhang, L., 2016. Molecular basis for adaptation of oysters to stressful marine intertidal environments. Annu. Rev. Anim. Biosci. 4, 357–381.

Zhou, Z., Wang, L., Yang, J., Zhang, H., Kong, P., Wang, M., Qiu, L., Song, L., 2011. A dopamine β hydroxylase from *Chlamys farreri* and its induced mRNA expression in the haemocytes after LPS stimulation. Fish Shellfish Immunol. 30, 154–162.